

Technical Note

Cine Flow Measurements Using Phase Contrast With Undersampled Projections: In Vitro Validation and Preliminary Results In Vivo

Andrew L. Wentland, BS,^{1–3*} Frank R. Korosec, PhD,^{1,2} Karl K. Vigen, PhD,^{1,2} Oliver Wieben, PhD,^{1,2} Jason P. Fine, PhD,⁴ and Thomas M. Grist, MD^{1–3}

Purpose: To assess the accuracy of flow measurements in vitro and in vivo during scan times shorter than a breath-hold using a 2D cine phase contrast (PC) undersampled radial acquisition method, which may be useful for measuring flow, especially in vessels subject to motion during respiration.

Materials and Methods: For in vitro assessment, a flow phantom was imaged at various flow rates and undersampling factors. For in vivo assessment, five normal subjects were imaged and the flow rate in the aorta was compared with the sum of the flow rates in the iliac arteries.

Results: For results in vitro, the accuracy of flow measurements was maintained with scan times as low as 13–17 seconds. For results in vivo, scans acquired in less than 25 seconds provided flow measurements in the aorta that corresponded well to the sum of flow measurements in the iliac arteries.

Conclusion: The undersampled radial acquisition cine PC technique provided accurate flow measurements in a flow phantom and in healthy human volunteers in scan times shorter than a typical breath-hold.

Key Words: phase contrast; projection reconstruction; flow imaging; fast magnetic resonance imaging; undersampling; radial acquisition

J. Magn. Reson. Imaging 2006;24:945–951.
© 2006 Wiley-Liss, Inc.

PHASE CONTRAST (PC) methods permit the in vivo measurement of blood velocities (1–3). With a slice oriented orthogonal to a vessel of interest, volume flow rate can be computed for through-plane flow (4,5). If the MR acquisition is synchronized to the heartbeat, volume flow rates can be determined throughout the cardiac cycle (6,7). Such quantitative measures can assist in the diagnosis of vascular diseases.

For example, Schoenberg et al (8) showed that MR PC flow measurements and the shape of the flow waveform throughout the cardiac cycle could be used to identify the hemodynamic significance of vascular pathologies in the renal arteries. However, they concluded that a higher temporal resolution than that achievable with commercially available MR flow measurement methods was needed to provide a more accurate demonstration of the flow waveform. Prince et al (9) sought to use non-cine 3D PC MR angiography (MRA) to assess the severity of stenoses, and found a marked correlation between hemodynamic significance and signal dephasing. However, PC used in this way provides a qualitative approach for assessing hemodynamic significance. Segmented EPI has been used to increase temporal resolution; however, this technique uses multiecho readout trains that lead to susceptibility-induced signal loss and distortions (10).

The accurate measurement of flow requires high spatial resolution for a true depiction of the cross-sectional area of the vessel of interest (11). In addition, a high temporal resolution is required for an accurate representation of the varying shape of a flow waveform throughout the cardiac cycle. Increased spatial resolution is typically obtained at the expense of a lower temporal resolution or longer scan time. Similarly, increased temporal resolution is typically achieved at the expense of a decreased spatial resolution or longer scan time.

When regions of the body that are affected by respiratory motion are scanned, the MR scan must accommodate the motion that can occur. Most frequently such examinations are performed during a single breath-hold in order to prevent motion-induced artifacts and blurring. Scans in these regions are limited to the duration of a patient's breath-hold (usually less

¹Department of Radiology, University of Wisconsin Medical School, Madison, Wisconsin, USA.

²Department of Medical Physics, University of Wisconsin Medical School, Madison, Wisconsin, USA.

³Department of Biomedical Engineering, University of Wisconsin, Madison, Wisconsin, USA.

⁴Department of Statistics, University of Wisconsin, Madison, Wisconsin, USA.

Contract grant sponsor: NIH; Contract grant number: HL67029.

*Address reprint requests to: A.L.W., J5/MISO CSC Medical Physics, Box 1590, 600 Highland Ave., Madison, WI 53792.
E-mail: alwentland@wisc.edu

Received July 15, 2005; Accepted June 29, 2006.

DOI 10.1002/jmri.20715

Published online 12 September 2006 in Wiley InterScience (www.interscience.wiley.com).

than 20–30 seconds), and therefore spatial resolution, temporal resolution, or both are typically compromised. This holds particularly true for PC imaging, since one reference data set must be acquired in addition to the data sets required for each flow-encoding direction. An alternative method to breath-hold imaging uses a navigator echo for a free-breathing acquisition (12).

Barger et al (13) developed a non-cine PC acquisition using azimuthally undersampled projections, or radial lines in k -space, that provides higher spatial resolution per unit time than a traditional spin-warp encoding technique. In high-contrast environments, such as those found in PC MRA, resolution does not firmly depend on the number of radial lines sampled. For a given scan time, images with better spatial and/or temporal resolution can be acquired using PC with undersampled projections (PC-PR). Alternatively, PC-PR can be used to reduce the total scan time without decreasing the spatial and/or temporal resolution. Although azimuthal undersampling does not decrease the spatial resolution, it does introduce streak artifacts (14) that in most cases are tolerable when the number of signal-generating objects in the field of view (FOV) is limited and the signal-to-noise ratio (SNR) of these objects is high. The intensity of streak artifacts increases with the amount of undersampling (15).

We developed a cardiac-triggered cine version of PC-PR to rapidly acquire a high spatial and temporal resolution 2D data set with the goal of obtaining accurate measurements of flow waveforms in the renal arteries of patients with renal artery stenosis. The purpose of this study was to validate PC-PR by assessing the accuracy of controlled in vitro flow measurements and determining the feasibility of obtaining accurate flow measurements in human subjects. Although our ultimate goal is to measure flow in the renal arteries, in this study we evaluated PC-PR in vivo by comparing the flow rate in the aorta with the sum of flow rates in the iliac arteries, since the sum of flow rates in the iliac arteries should equal the flow rate in the aorta.

MATERIALS AND METHODS

In Vitro Studies

The undersampled and cardiac-triggered cine PC-PR sequence was implemented on a 1.5 T MR scanner (Signa Excite, GE Healthcare, Milwaukee, WI, USA). Figure 1 demonstrates how the projections were acquired. Projection pairs with and without bipolar gradients were acquired sequentially in time at the identical projection angle for velocity encoding. Data acquisition was segmented such that one or two projections, or radial k -space lines, were acquired per segment (views per segment (vps)). One segment was acquired per simulated cardiac cycle. Each segment was repeatedly acquired as many times as possible within each simulated cardiac cycle. The data were reconstructed into images representing information at different time points (phases or frames) throughout the simulated cardiac cycle.

For in vitro assessment, the PC-PR method was used to image blood-mimicking fluid that was being pumped

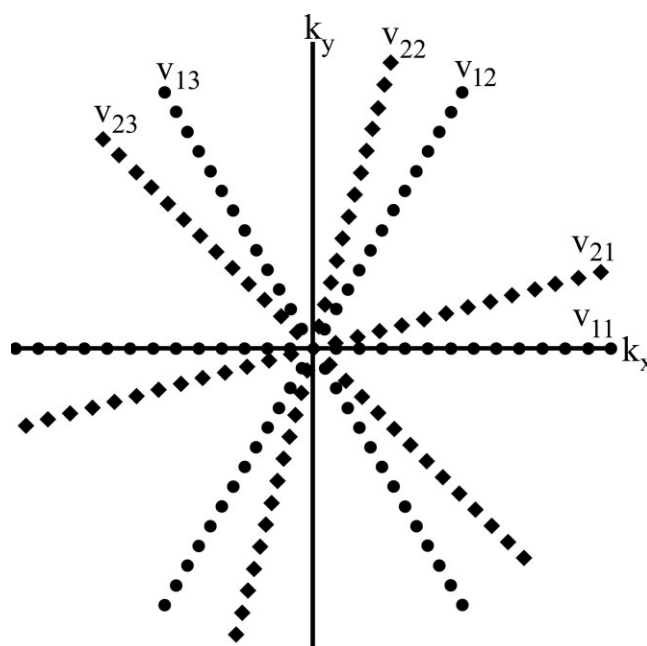
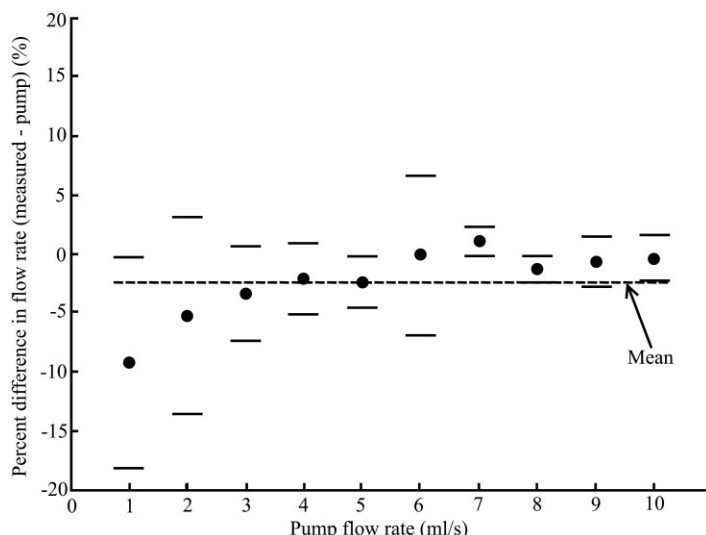


Figure 1. k -Space diagram demonstrating azimuthal undersampling. Projections v_{ij} for a single cardiac phase or frame are acquired in an interleaved fashion (where i represents the interleave index (the RR interval during which the projections are acquired), and j is the projection index within the interleaf). Each projection is sampled twice before the projection angle is incremented (once using a bipolar gradient to velocity-encode the echo, and once without the bipolar gradient for a reference). Undersampled areas in the outer regions of k -space lead to streak artifacts but do not substantially compromise the spatial resolution of the reconstructed image. Oversampling the center of k -space mitigates motion and pulsatility artifacts.

through a 0.635-cm inner diameter tube by a computer-controlled flow pump (100060 UHDC Flow System; R.G. Shelley Ltd., Toronto, Canada) with an accuracy of $\pm 1\%$ according to the pump manufacturer. A four-element phased-array torso coil (GE Healthcare, Milwaukee, WI, USA) was employed for through-plane flow measurements and the following imaging parameters were used: TR/TE = 6.4/3.0 msec, BW = ± 31.25 kHz, FOV = 24–34 cm, slice thickness = 5 mm, flip angle = 30° , and 256 data samples along each projection. Data were acquired during constant flow and sinusoidal flow. The former was triggered at 60 beats per minute (bpm) using a waveform generator (M310 ECG Simulator; Fogg System Company, Inc., Denver, CO, USA), and the latter was triggered at 60 bpm using a signal generated by the pump. Scans were performed with eight, 16, 32, 64, 128, and 256 projections for constant and sinusoidal flow rates of 1–10 mL/second in 1-mL/second intervals for scan times ranging from four to 120 seconds. Sinusoidal flow waveforms were designed to have a DC offset corresponding to each average flow rate, and the flow varied ± 1 mL/second about each average flow rate. Scans were repeated three times at each flow rate and with each of the specified number of projections. Images were reconstructed offline. The projection data were regridded using a Kaiser-Bessel interpolation kernel of ± 2 pixels. The regridded data were

Figure 2. Bland-Altman analysis of scans of constant flow through a phantom acquired using PC-PR with 64 projections. The percent differences between the average measured flow rates and the pump's flow rate are shown on the ordinate, while the pump's flow rates are shown on the abscissa. Three scans were performed at each flow rate for averaging and error calculations. Error bars are shown (mean \pm 2 SD). The mean percent difference across all flow rates was -2.35% .



then inverse Fourier transformed, and phase difference and magnitude images were produced. The phase difference data from the four coil elements were combined using the hybrid method described by Bernstein et al (17).

The images were subsequently analyzed with a commercial flow analysis package (CV Flow; Medis, The Netherlands). Regions of interest (ROIs) were drawn on each of the magnitude images and automatically copied onto the corresponding phase difference images by the software. ROIs were propagated across all phases. Flow data were generated by the software and recorded for analysis.

Finally, we summarized the data using Bland-Altman analysis (16) and compared the known flow rate of the pump with the measured flow rate from the images acquired with the PC-PR method. The data used in the analysis were averages of flow measurements acquired from the three repeated scans and all of the flow measurements acquired throughout the simulated cardiac cycle.

Human In Vivo Studies

Evaluations in vivo were performed on five normal subjects (three males and two females, mean age = 40 ± 15 years) with parameters similar to those described above. Informed consent was obtained prior to each examination. Images were acquired during breath-hold intervals as long as 25 seconds (64 projections) and as short as four seconds (eight projections). In each of the human subjects three data sets were acquired: one oriented orthogonal to the flow in the aorta, a second oriented orthogonal to the flow in the left iliac artery, and a third oriented orthogonal to the flow in the right iliac artery. The three scans were performed in each subject using 64, 32, 16, and eight projections, and repeated with one and two vps. Images were also acquired with a traditional cardiac-gated, segmented spin-warp PC acquisition method with TR/TE = 9.9/4.4 msec, two vps, BW = ± 31.25 kHz, flip angle = 45° , 28–35 seconds per scan using 128 phase-encoding values, and a half FOV. Data were acquired using a four-

element phased-array torso coil. A spin-warp acquisition with one vps required too long a scan time to be completed during a breath-hold, and therefore it was not attempted. Data were tabulated to compare the flow rate in the aorta with the sum of the flow rates in the iliac arteries. The *P*-values from a paired *t*-test with a significance level of 0.05 were computed from the tabulated data to compare flow measurements obtained from the PC-PR and spin-warp acquisitions.

RESULTS

In Vitro Studies

Images of constant flow through the phantom (flow rates of 1–10 mL/second in 1-mL/second increments), acquired in 34 seconds using 64 projections, yielded flow measurements that were on average 2.35% lower than the actual flow rates of the pump (Fig. 2). Scans using other undersampling factors yielded average percent differences of -1.97% using 32 projections, -9.13% using 16 projections, and -16.01% using eight projections (Table 1). For scans acquired in times longer than an average breath-hold, the average percent difference was -1.89% using 128 projections and -0.82% using 256 projections (Table 1). Images of pulsatile flow through the phantom (average flow rates of 1–10 mL/second in 1-mL/second increments) yielded flow measurements averaging percent differences of $+0.45\%$ using 256 projections, $+0.08\%$ using 128 projections, $+1.09\%$ using 64 projections, $+1.52\%$ using 32 projections, $+6.57\%$ using 16 projections, and $+13.47\%$ using eight projections (Table 2). Images of pulsatile flow acquired with PC-PR using eight, 16, 32, and 256 projections are shown in Fig. 3a.

Human In Vivo Studies

Scans acquired using 32 projections and one vps (used to evaluate the potential benefit of improved temporal resolution) yielded flow measurements with accuracies similar to those obtained using PC-PR with two vps. Average flow rates were calculated using all of the im-

Table 1
Constant Flow*

| Average flow rate (mL/second) | % Difference \pm 2 SD (mL/second) for various numbers of projections | | | | | |
|----------------------------------|--|------------------|------------------|-------------------|--------------------|--------------------|
| | $N_p = 256$ | $N_p = 128$ | $N_p = 64$ | $N_p = 32$ | $N_p = 16$ | $N_p = 8$ |
| 1 | -0.68 ± 3.12 | -7.53 ± 8.26 | -9.20 ± 8.91 | -8.07 ± 11.04 | -34.35 ± 11.67 | -39.47 ± 13.81 |
| 2 | -0.91 ± 2.12 | -4.33 ± 4.77 | -5.20 ± 8.32 | -4.40 ± 5.20 | -17.98 ± 5.94 | -26.33 ± 5.09 |
| 3 | -2.09 ± 1.20 | -1.44 ± 2.85 | -3.36 ± 3.97 | -3.22 ± 1.89 | -13.93 ± 9.34 | -19.02 ± 1.90 |
| 4 | -1.80 ± 1.57 | -2.57 ± 3.13 | -2.10 ± 2.95 | -0.17 ± 0.31 | -6.93 ± 7.13 | -13.71 ± 4.05 |
| 5 | -1.05 ± 2.49 | -3.96 ± 1.32 | -2.37 ± 2.14 | -0.64 ± 1.29 | -7.29 ± 6.06 | -13.66 ± 1.79 |
| 6 | -1.12 ± 2.50 | -2.24 ± 3.04 | -0.10 ± 6.74 | -0.44 ± 1.24 | -4.58 ± 5.84 | -11.13 ± 6.89 |
| 7 | -0.70 ± 1.69 | $+0.15 \pm 1.03$ | $+1.07 \pm 1.21$ | -0.20 ± 0.47 | -1.92 ± 8.66 | -13.46 ± 9.70 |
| 8 | $+0.29 \pm 1.93$ | $+1.13 \pm 1.06$ | -1.28 ± 1.15 | -0.67 ± 1.15 | -1.66 ± 2.20 | -8.25 ± 3.45 |
| 9 | -0.13 ± 0.53 | $+1.10 \pm 1.97$ | -0.64 ± 2.06 | -1.48 ± 2.46 | -1.82 ± 4.25 | -7.46 ± 2.80 |
| 10 | -0.04 ± 0.71 | $+0.81 \pm 1.48$ | -0.36 ± 1.91 | -0.37 ± 1.40 | -0.83 ± 0.97 | -7.60 ± 6.50 |

*Average percent differences between the average measured flow rates calculated using images acquired with PC-PR and the known flow rate of the pump.

N_p = number of projections, SD = standard deviation.

ages acquired during the RR interval, with 40–45 phases collected with PC-PR scans at one vps, 20–22 phases collected with PC-PR scans at two vps, and 13 phases acquired with the traditional spin-warp acquisition at two vps. Images acquired in vivo using PC-PR are shown in Fig. 3b and c. Even though there are significant streak artifacts in the magnitude images emanating from high signal in the abdominal wall, these artifacts are not present in the phase difference images since the abdominal wall does not move during the acquisition. Note that the imaging time required for the spin-warp acquisition with 128 phase-encoding values, two vps, and a half FOV was the same time required for the PC-PR acquisition using 32 projections, one vps, and a whole FOV. Since the SNR and CNR of images acquired using PC-PR with eight and 16 projections were inadequate, no flow rates were measured when these parameters were used in vivo.

The difference between the flow rate in the aorta and the summed flow rates in the iliac arteries was calculated for each method. A paired *t*-test revealed a significant difference (P -value < 0.05 [$P = 0.02$]) between measurements obtained using the PC-PR acquisition with 32 projections and one vps, and the spin-warp method acquired using 128 phase-encoding values and two vps. Similarly, a significant difference (P -value $<$

0.05 [$P = 0.0003$]) was determined between measurements obtained using the PC-PR acquisition with 64 projections and two vps, and the spin-warp method acquired using 128 phase-encoding values and two vps. Finally, a P -value > 0.05 ($P = 0.72$) was computed when data from undersampled PC-PR were paired using one and two vps, and therefore no significant difference between PC-PR using one or two vps was established. Figure 4 shows the results of these paired *t*-tests along with a bar graph showing the mean difference between the flow rate in the aorta and the summed flow rates in the iliac arteries for the three acquisition methods.

DISCUSSION

The maximum average breath-hold duration for the subjects was about 30 seconds. The in vitro PC-PR results show that accurate flow rates were obtained within scan times as short as 13–17 seconds for an acquisition using 32 projections and two vps, and demonstrate that PC-PR is a useful method for obtaining accurate flow measurements even in individuals with limited breath-holding ability. For individuals who can hold their breath for 30 seconds or longer, PC-PR provides the option to reduce streak artifacts by acquiring

Table 2
Pulsatile Flow*

| Average flow rate (mL/second) | % Difference \pm 2 SD (mL/second) for various numbers of projections | | | | | |
|----------------------------------|--|------------------|-------------------|-------------------|-------------------|--------------------|
| | $N_p = 256$ | $N_p = 128$ | $N_p = 64$ | $N_p = 32$ | $N_p = 16$ | $N_p = 8$ |
| 1 | $+1.41 \pm 6.66$ | $+0.27 \pm 7.59$ | $+4.67 \pm 18.01$ | $+6.60 \pm 35.00$ | $+26.01 \pm 3.89$ | $+49.10 \pm 15.20$ |
| 2 | $+0.95 \pm 3.55$ | $+0.71 \pm 5.76$ | $+2.71 \pm 4.01$ | $+5.20 \pm 11.70$ | $+13.01 \pm 6.92$ | $+11.55 \pm 5.00$ |
| 3 | $+0.61 \pm 2.75$ | -0.12 ± 2.55 | $+1.25 \pm 2.69$ | $+0.68 \pm 6.64$ | $+5.07 \pm 5.22$ | $+14.40 \pm 10.00$ |
| 4 | $+0.92 \pm 1.86$ | -0.09 ± 1.74 | $+1.14 \pm 2.66$ | -2.28 ± 3.70 | $+5.77 \pm 7.88$ | $+22.28 \pm 5.30$ |
| 5 | $+0.04 \pm 0.44$ | $+0.10 \pm 2.72$ | -0.40 ± 1.18 | $+0.84 \pm 6.03$ | $+9.84 \pm 3.52$ | $+13.44 \pm 1.28$ |
| 6 | $+0.11 \pm 1.22$ | -0.18 ± 1.72 | -0.36 ± 1.50 | $+1.60 \pm 5.40$ | $+1.36 \pm 5.92$ | $+1.97 \pm 4.33$ |
| 7 | $+0.20 \pm 0.76$ | -0.24 ± 1.78 | $+0.39 \pm 1.02$ | $+1.01 \pm 3.17$ | $+1.49 \pm 4.72$ | $+3.99 \pm 1.60$ |
| 8 | $+0.22 \pm 0.87$ | $+0.81 \pm 0.74$ | $+0.09 \pm 1.42$ | -0.33 ± 0.82 | -0.74 ± 0.90 | $+6.20 \pm 7.75$ |
| 9 | $+0.37 \pm 0.89$ | $+0.19 \pm 0.90$ | $+0.62 \pm 1.03$ | $+0.70 \pm 2.21$ | $+1.81 \pm 1.32$ | $+6.01 \pm 2.04$ |
| 10 | -0.31 ± 0.82 | -0.64 ± 2.30 | $+0.82 \pm 0.65$ | $+1.12 \pm 1.15$ | $+2.04 \pm 0.37$ | $+5.76 \pm 4.62$ |

*Average percent differences between the average measured flow rates calculated using images acquired with PC-PR and the known flow rate of the pump.

N_p = number of projections, SD = standard deviation.

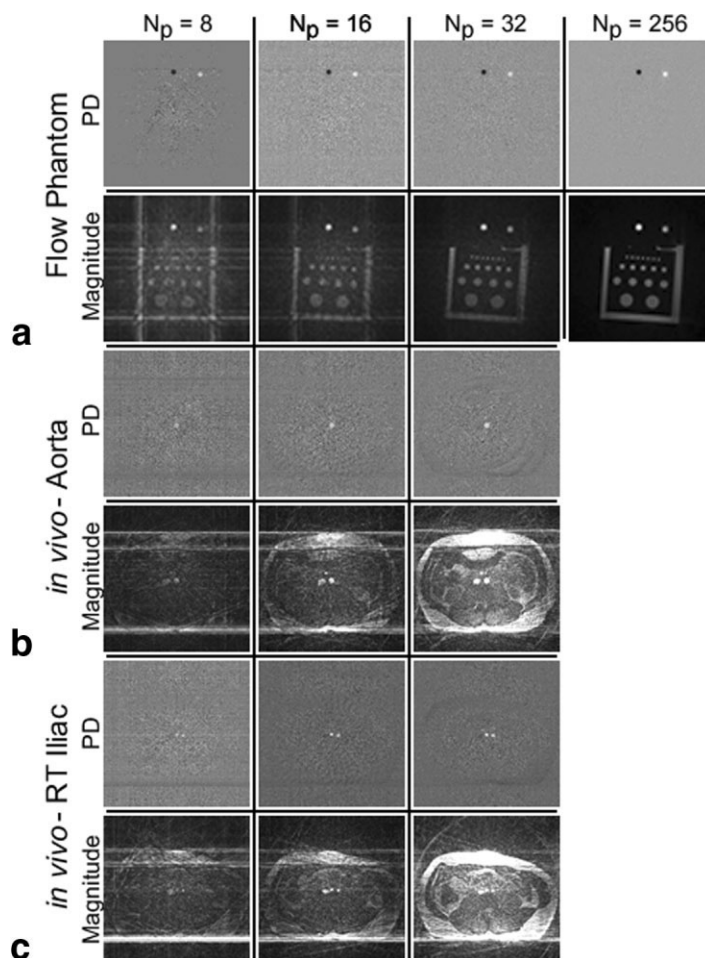


Figure 3. Phase difference and magnitude images acquired using PC-PR. **a:** Cross-sectional in vitro images showing one phase of pulsatile flow through the phantom acquired using eight, 16, 32, and 256 projections. (A resolution phantom used to simulate stationary tissue appears in the magnitude images.) **b:** Cross-sectional in vivo images showing one phase of flow through the aorta acquired using eight, 16, and 32 projections. **c:** Cross-sectional images showing one phase of flow through the right iliac artery acquired using eight, 16, and 32 projections. All images were acquired using two vps. RT = right, PD = phase difference, N_p = number of projections.

64 projections and two vps, or to improve temporal resolution by acquiring 32 projections and one vps. Therefore, the PC-PR acquisition is useful for reducing scan time without diminishing the integrity of flow measurements and may be particularly useful for imaging

individuals who cannot hold their breath for an extended period of time.

Overall, the in vitro flow measurements obtained using the PC-PR acquisition method and scans acquired with as few as 32 projections were accurate. In fact, the

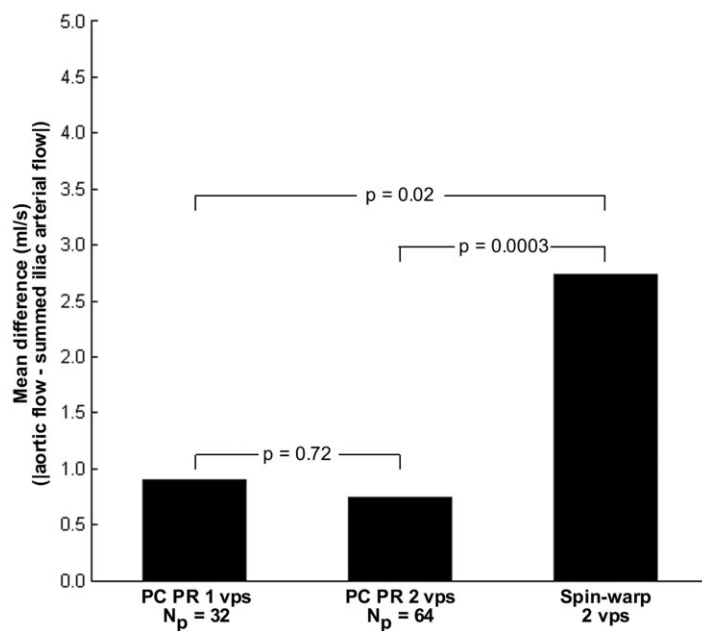


Figure 4. Mean difference in flow rates between aortic flow and the summed flow rates in the right and left iliac arteries as measured from PC-PR scans acquired with one and two vps, along with the mean difference in measurements obtained using a cardiac-gated spin-warp PC acquisition with two vps. P -values obtained using a paired t -test with a significance level of 0.05 are shown to compare the differences between each method.

magnitude of the error in the flow measurements was consistently within a few tenths of 1 mL/second of the average flow rate. As a result, as shown in Fig. 2, the percent differences in the flow measurements obtained using flow rates of ≤ 2 mL/second were larger than those obtained at higher flow rates. With an FOV of 24–34 cm and 256 data samples along each projection, a voxel dimension of 0.9 to 1.3 mm were obtained. When imaging smaller vessels, one can improve the spatial resolution by increasing the number of sample points along each projection to 512, which will result in only a minimal increase in scan time due to the increase in TR.

There tended to be greater variation in the in vivo flow measurements using the traditional spin-warp acquisition compared to the PC-PR acquisition. Using the spin-warp method, the flow measurement from the aorta was different from the summed flow measurements from the two iliac arteries. For the PC-PR acquisition using 32 and 64 projections, the flow rates were similar between the aorta and iliac arteries. Although the true flow rates in the vessels were unknown, the flow measurements acquired using PC-PR provided more consistent results. Low spatial resolution may account for the inaccurate flow measurements obtained using the spin-warp acquisition. It has been demonstrated that flow measurements will be inaccurate if an insufficient number of pixels spans the vessel of interest (11).

Paired *t*-tests demonstrated a significant difference in the in vivo measurements obtained using the spin-warp and PC-PR methods. On the contrary, paired *t*-test results showed no significant difference between measurements obtained using the PC-PR acquisition with one or two vps. Although a *t*-test cannot characterize the similarity of the measured flow rate in the aorta to the sum of the measured flow rates in the iliac arteries, this statistical test does show the marked difference between the results obtained using the PC-PR method and the traditional spin-warp method. Although not indicated by the statistics, the PC-PR acquisition with one vps provides improved temporal resolution vs. the PC-PR acquisition with two vps. This improved temporal resolution may be useful for detecting the peak flow during the RR interval. The minimum TRs were used for both the spin-warp and PC-PR acquisitions. Since radial acquisitions do not need a phase-encoding gradient, the PC-PR method had a lower minimum TR than the spin-warp acquisition.

In general, undersampled radial acquisitions, such as PC-PR, are limited by streak artifacts introduced by undersampling. Although these artifacts tend to emanate out of and away from the vessels of interest, their appearance may render the image difficult to analyze. In addition, the definition of vessel boundaries in the magnitude images can become more challenging and affect the ROI placement. Vessels exhibiting pulsatility generate the most noticeable streak artifacts. The cardiac-gated acquisition used in this study mitigated some of the pulsatility effects and allowed for a further reduction in the number of projections than was previously possible (13). Streak artifacts are worse when fewer projections are used. By limiting the minimum number of projections to 32, the effects of streaks on

adjacent vessels can be minimized. Nevertheless, reasonable results were obtained using eight and 16 projections.

The PC-PR method has shown promising results for accurate flow measurements in healthy volunteers. Although our ultimate goal is to apply the PC-PR technique to the renal arteries, we chose to use the aorta and iliac arteries to obtain an intrinsic validation in humans. In an ongoing study, we are using the PC-PR method to measure the flow rates in the renal arteries of swine during a forced breath-hold to evaluate the feasibility of detecting the hemodynamic significance of renal artery stenoses.

In future studies it may be advantageous to compare the PC-PR technique with spin-warp PC methods that employ parallel imaging to achieve reductions in scan time by factors of 2 or 4. A non-Cartesian sensitivity encoding (SENSE) method was previously implemented by Pruessmann et al (18). Therefore, future studies could include comparisons between PC-PR and spin-warp PC methods that use parallel imaging.

In conclusion, we have shown that the PC-PR technique provides accurate and reproducible flow measurements in vitro in shorter scan times than an average breath-hold. The results from healthy normal volunteers are promising. Depending on the ability of a patient to perform a breath-hold, PC-PR may be used to reduce the scan time without compromising the accuracy of flow measurements. PC-PR may be useful in the future for imaging renal flow and assessing the hemodynamic significance of stenoses.

ACKNOWLEDGMENT

The authors thank Kelli Hellenbrand for her help in scanning the volunteers.

REFERENCES

1. Moran PR. A flow velocity zeugmatographic interlace for NMR imaging in humans. *Magn Reson Imaging* 1982;1:197–203.
2. Pelc NJ, Bernstein MA, Shimakawa A, Glover GH. Encoding strategies for three-direction phase-contrast MR imaging of flow. *J Magn Reson Imaging* 1991;1:405–413.
3. Hausmann R, Lewin JS, Laub G. Phase-contrast MR angiography with reduced acquisition time: new concepts in sequence design. *J Magn Reson Imaging* 1991;1:415–422.
4. Pelc NJ, Sommer FG, Li KC, Brosnan TJ, Herfkens RJ, Enzmann DR. Quantitative magnetic resonance flow imaging. *Magn Reson Q* 1994;10:125–147.
5. Firmin DN, Nayler GL, Kilner PJ, Longmore DB. The application of phase shifts in NMR for flow measurement. *Magn Reson Med* 1990;14:230–241.
6. Nayler GL, Firmin DN, Longmore DB. Blood flow imaging by cine magnetic resonance. *J Comput Assist Tomogr* 1986;10:715–722.
7. Rebergen SA, van der Wall EE, Doornbos J, de Roos A. Magnetic resonance measurement of velocity and flow: technique, validation, and cardiovascular applications. *Am Heart J* 1993;126:1439–1456.
8. Schoenberg SO, Knopp MV, Bock M, et al. Renal artery stenosis: grading of hemodynamic changes with cine phase-contrast MR blood flow measurements. *Radiology* 1997;203:45–53.
9. Prince MR, Schoenberg SO, Ward JS, Londy FJ, Wakefield TW, Stanley JC. Hemodynamically significant atherosclerotic renal artery stenosis: MR angiographic features. *Radiology* 1997;205:128–136.
10. McKinnon GC. Interleaved echo planar phase contrast angiography. *Magn Reson Med* 1994;31:682–685.

11. Tang C, Blatter DD, Parker DL. Accuracy of phase-contrast flow measurements in the presence of partial-volume effects. *J Magn Reson Imaging* 1993;3:377–385.
12. Wang Y, Rossman PJ, Grimm RC, Riederer SJ, Ehman RL. Navigator-echo-based real-time respiratory gating and triggering for reduction of respiration effects in three-dimensional coronary MR angiography. *Radiology* 1996;198:55–60.
13. Barger AV, Peters DC, Block WF, et al. Phase-contrast with interleaved undersampled projections. *Magn Reson Med* 2000;43:503–509.
14. Peters DC, Korosec FR, Grist TM, et al. Undersampled projection reconstruction applied to MR angiography. *Magn Reson Med* 2000;43:91–101.
15. Vigen KK, Peters DC, Grist TM, Block WF, Mistretta CA. Undersampled projection-reconstruction imaging for time-resolved contrast-enhanced imaging. *Magn Reson Med* 2000;43:170–176.
16. Bland JM, Altman DG. Statistical methods for assessing agreement between two methods of clinical measurement. *Lancet* 1986;1:307–310.
17. Bernstein MA, Grgic M, Brosnan TJ, Pelc NJ. Reconstructions of phase contrast, phased array multicoil data. *Magn Reson Med* 1994;32:330–334.
18. Pruessmann KP, Weiger M, Bornert P, Boesiger P. Advances in sensitivity encoding with arbitrary k -space trajectories. *Magn Reson Med* 2001;46:638–651.